Electronic Supplementary Information

Dendritic porous copper foam-carbonic anhydrase biohybrid for carbon dioxide electroreduction

Minli Shu,[a] Boqiang Miao,[b] Siqi Zhang,[a] Zhe Wang,[b] Xuefang Zhu,[a]* Yucheng Jiang [a]* and Yu Chen[b]

[a] *School of Chemistry & Chemical Engineering, Key Laboratory of Macromolecular Science of Shaanxi Province, Shaanxi Normal University, Xi'an 710119, China.*

[b] *School of Materials Science and Engineering, Shaanxi Normal University, Xi'an 710119, China.*

Corresponding authors:

E-mail: jyc@snnu.edu.cn (Y. Jiang), zhuxuefang@snnu.edu.cn (X. Zhu)

1. Experimental section

Reagents and chemicals: Anhydrous cupric sulfate ($CuSO_4 \cdot 5H_2O$, 99%), sulfuric acid (H_2SO_4, 98%), hydrochloric acid (HCl, 38%), potassium dihydrogen phosphate (KH_2PO_4, 99%), dipotassium hydrogen phosphate (K_2HPO_4, 99%), deuterium oxide (D_2O 99%), ethanol (C_2H_6O, 99%), potassium bicarbonate ($KHCO_3$, 99%), dimethyl sulfoxide-d_6 (DMSO-d_6, 99%), tris (Hydroxymethyl) aminomethane hydrochloride ($(HOCH_2)_3CNH_2$, 99.8%) were obtained from Sinopharm Chemical Reagent Co., Ltd. (Shanghai, China). Carbonic anhydrase from bovine erythrocytes (CA, 95%), and EZBlue ($C_{45}H_{44}N_3NaO_7S_2$) were obtained from Sigma-Aldrich. All reagents in this work are analytically pure and can be used directly without further purification.

***Physical characterization*:** X-ray diffraction (XRD) patterns were recorded at a DX-2700 power X-ray diffractometer with a Cu Kα radiation source. X-ray photoelectron spectroscopy (XPS) spectra were obtained at an AXIS ULTRA spectrometer, and the binding energy was calibrated with a C1s peak at 284.6 eV as the standard value. Energy dispersive X-ray spectroscopy (EDX) was obtained at Quanta 200. Scanning electron microscopy (SEM) was investigated on a SU8220. Transmission electron microscopy (TEM), selected area electron diffraction (SAED), and TEM-EDX images were carried out on a JEM 2800.

Synthesis of 3D-Cu: To prepare 3D-Cu, 0.2 M $CuSO_4$ solution and 1.5 M H_2SO_4 solution were prepared.[1,2] The 1×1 cm^2 Cu sheet was immersed in the electrolyte, and the 80 s were deposited at different potentials (-1.0 V, -1.1 V, -1.2 V vs. reversible hydrogen electrode RHE) by a constant potential deposition method. The strong competitive reaction of hydrogen evolution results in the formation of porous dendritic Cu with uniform morphology and moderate size.

Electrochemical measurements: Electrochemical experiments were performed using a CHI 760E workstation with an H-type electrolytic cell separated with Nafion 117 membrane operating at room temperature. A silver/silver chloride (Ag/AgCl) was used as the reference electrode, the platinum sheet electrode was used as the opposite electrode, and the modified

electrode was used as the working electrode. The phosphate buffer solution (PBS, 0.1 M, 80 mL, pH=6.5) was divided evenly into cathodic and anodic compartments. Carbon dioxide was injected into the cathode for electrochemical reduction. All potentials in the work were correspond to the RHE, in which RHE = $E_{Ag/AgCl}$ + 0.197 V + 0.0591pH.[3]

Ultraviolet detection: The loading amounts of CA were measured by ultraviolet-visible spectrophotometer (UV-vis, Cary60). The protein content was measured by the Coomassie bright blue method. The content of CA before and after loading was compared and the enzyme loading was calculated.[4]

Product detection: Gaseous products including H_2, CO, etc were measured by gas chromatography on a zhejiangfili GC9700II equipped with two FID hydrogen flame ionization detectors and one TCD thermal conductivity cell detecto rand using N_2 as a carrier gas. The liquid phase products were detected by nuclear magnetic resonance (NMR; 400 MHz, JNM-ECZ400R/S1, JEOL) using 500 μL of reaction electrolyte and 100 μL of D_2O as solvent and 50 μL of DMSO-d_6 as internal standard.[5]

Computational methods:

The gas product is calculated by the following formula:

$$FE_{gas} = \frac{Z \times F \times V(mL\ min^{-1}) \times v(vol\ \%) \times P}{R \times T \times I_{total} \times 60(s\ min^{-1})} \quad (1)$$

where F is the Faraday constant (96485 C mol^{-1}), Z is the electron transfer number, V is the gas flow rate obtained using a flow meter (5 mL min^{-1}), P is one atmosphere (1.013×10^5 Pa), R is the universal gas constant (8.314 J mol^{-1} K^{-1}), I is the total steady-state cell current, and T is the room temperature (298.15 K).

The liquid phase product is calculated by the following formula:

$$FE_{HCOOH} = \frac{Z \times F \times n_{products}}{Q} \times 100\% \quad (2)$$

where Q denotes the total charge (C) and *products* denote the moles of the obtained formic acid calculated by ^{1}H-NMR.[6]

Figures

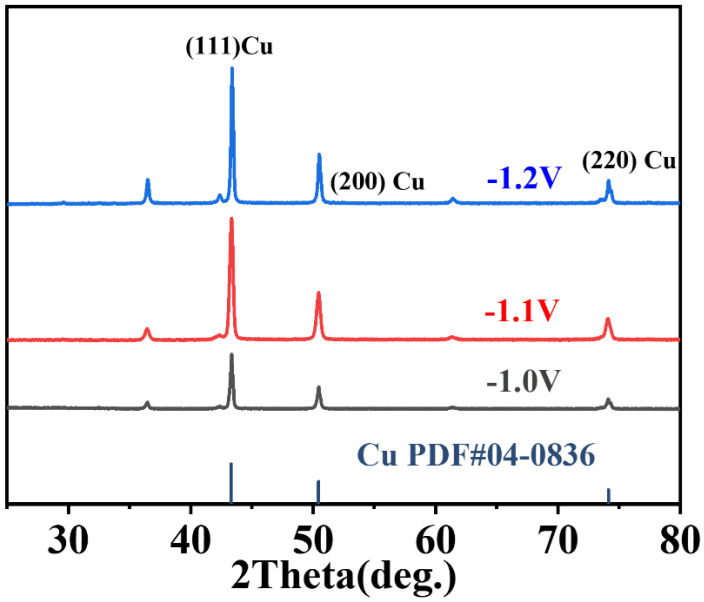

Fig. S1 XRD patterns of 3D-Cu obtained at different deposition potentials in 1.5 M H_2SO_4 solution containing 0.2 M $CuSO_4$ solution for 80 seconds.

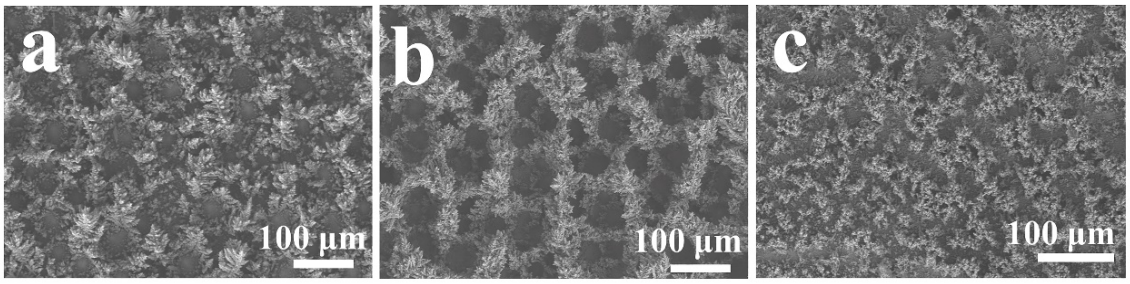

Fig. S2 SEM images of 3D-Cu at different deposition potentials (a) -1.0 V vs. RHE, (b) -1.1 V vs. RHE, (c) -1.2 V vs. RHE.

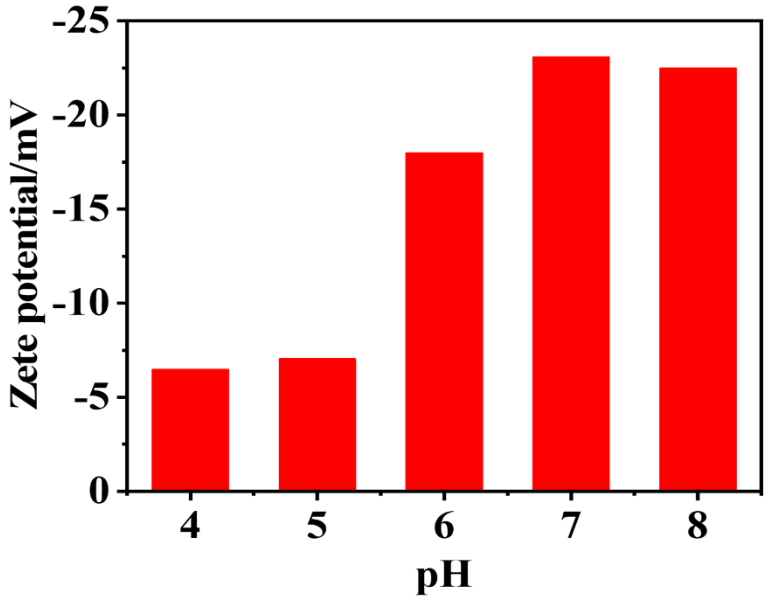

Fig. S3 Zeta potentials of 3D-Cu in PBS with different pH.

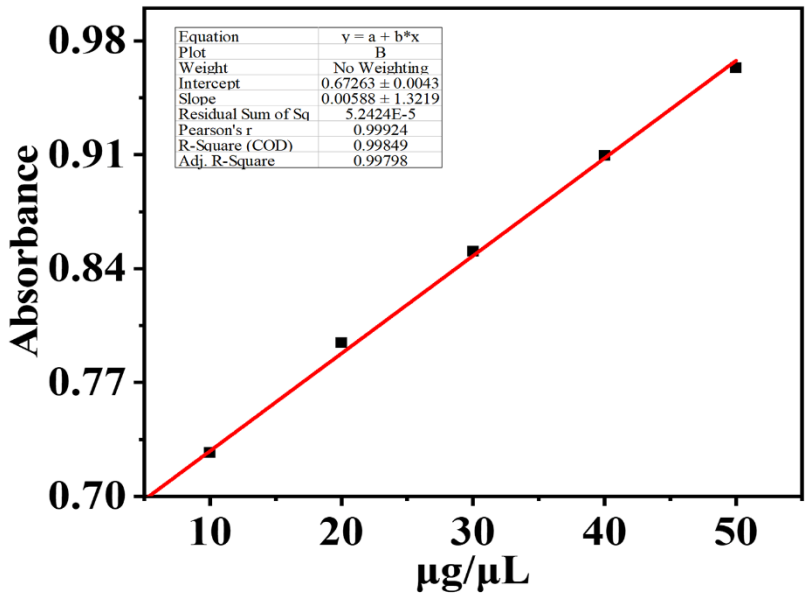

Fig. S4 Standard curves of different concentrations of CA versus UV-vis absorption.

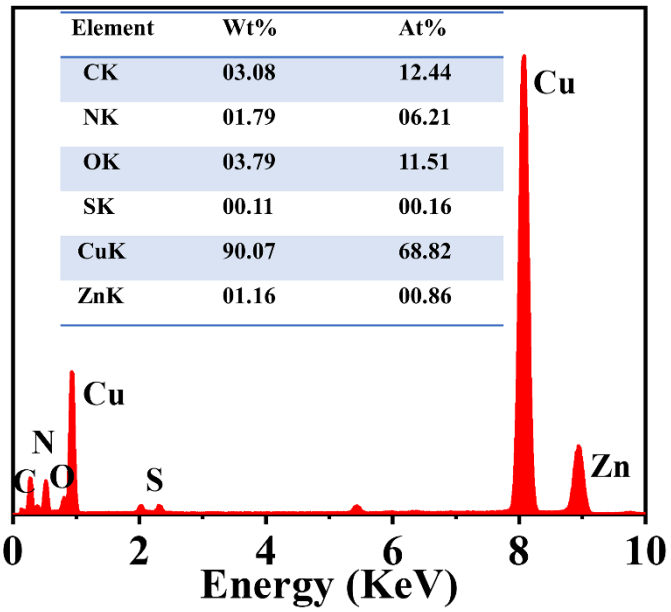

Fig. S5 EDX spectrum of CA/3D-Cu biohybrid.

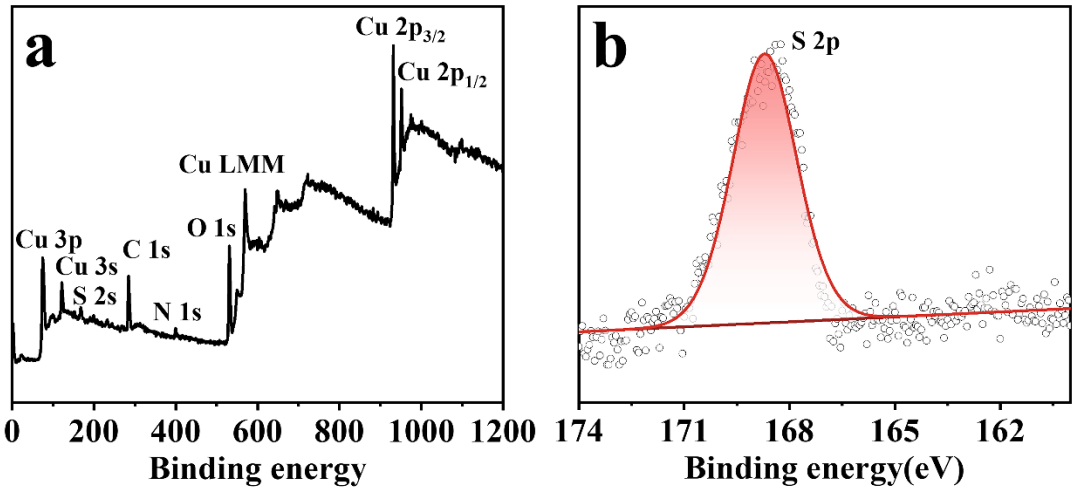

Fig. S6 (a) The full XPS spectrum and (b) S2p XPS spectrum of CA/3D-Cu biohybrid.

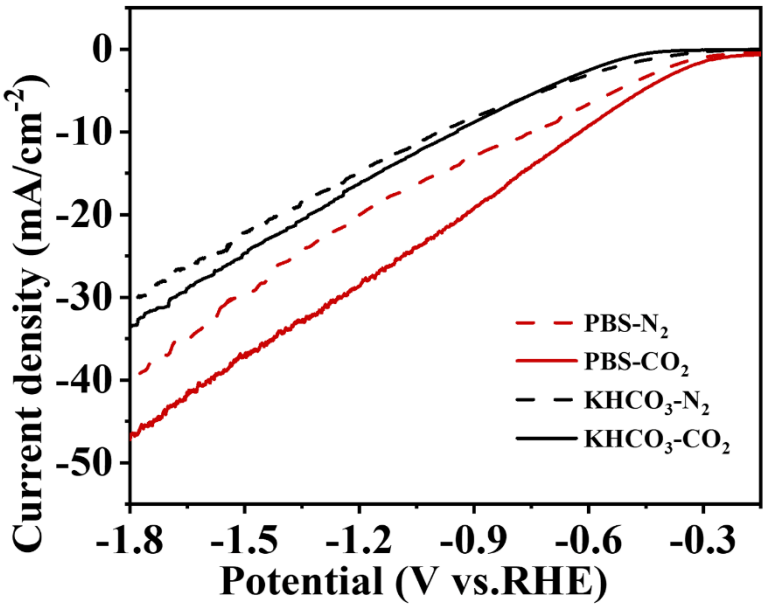

Fig. S7 LSV curves of CA/3D-Cu biohybrid in 0.1 M PBS or $KHCO_3$ at pH 6.5.

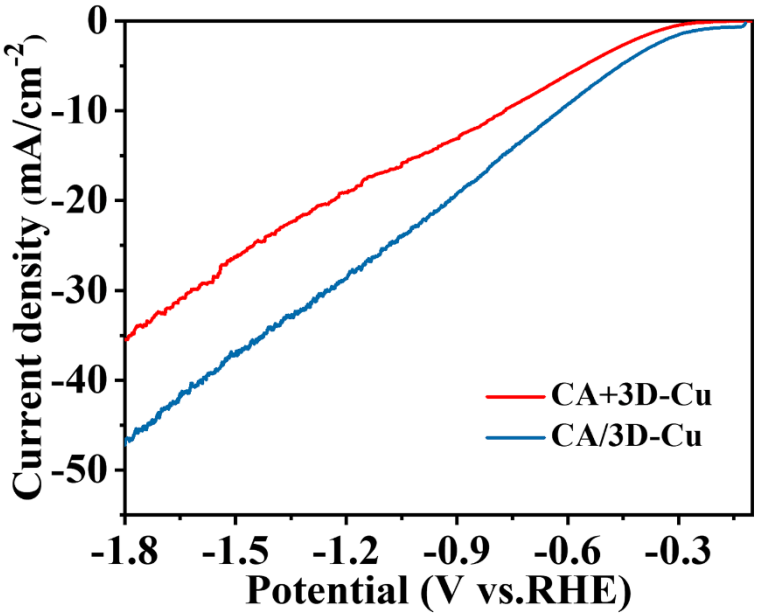

Fig. S8 LSV curves of 3D-Cu with 2.6 pmol CA in PBS and CA/3D-Cu biohybrid at pH 6.5.

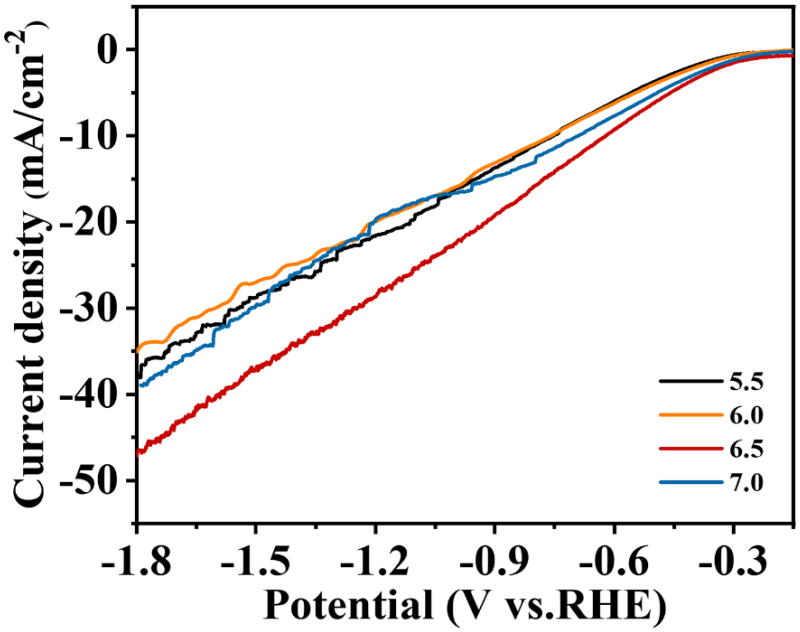

Fig. S9 LSV curves of CA/3D-Cu biohybrid in CO_2-saturated 0.1 M PBS with different pH.

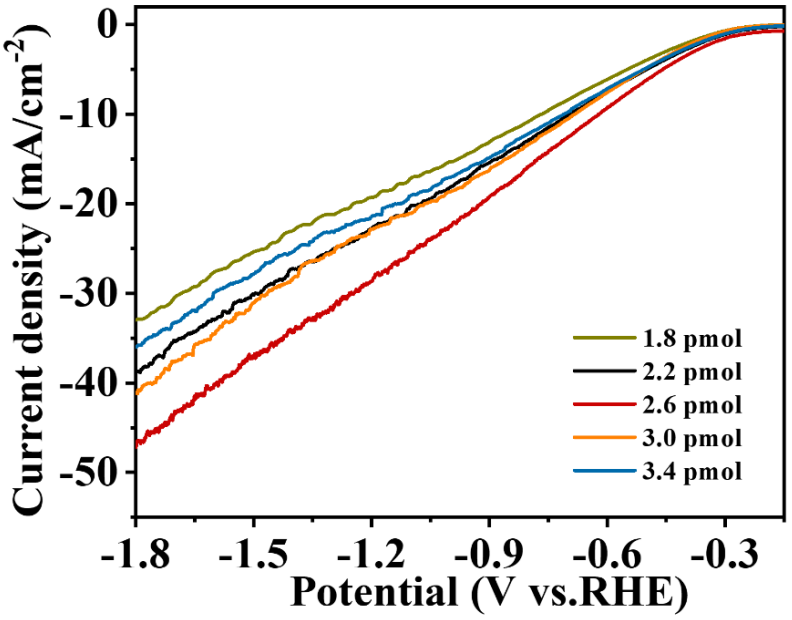

Fig. S10 LSV curves of CA/3D-Cu biohybrid with different CA content.

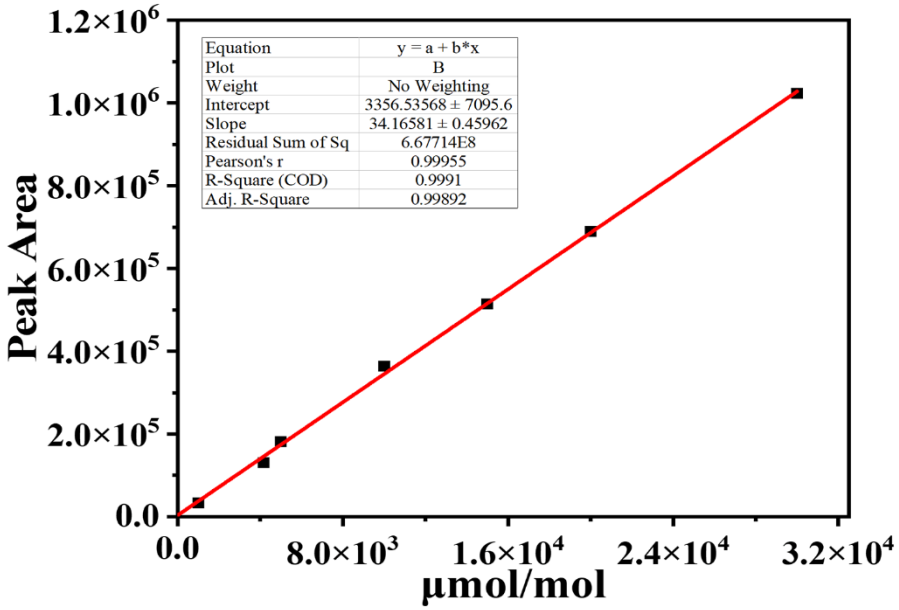

Fig. S11 Standard curve of H_2.

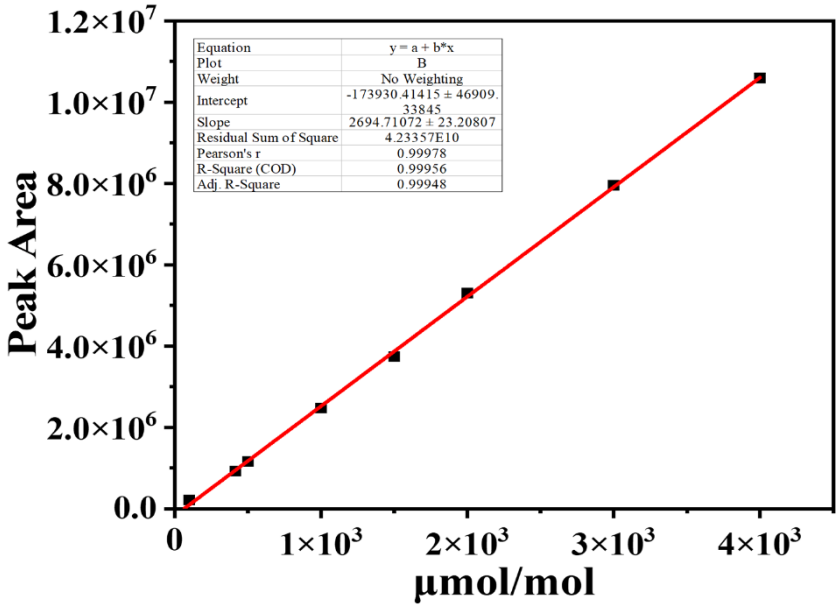

Fig. S12 Standard curve of CO.

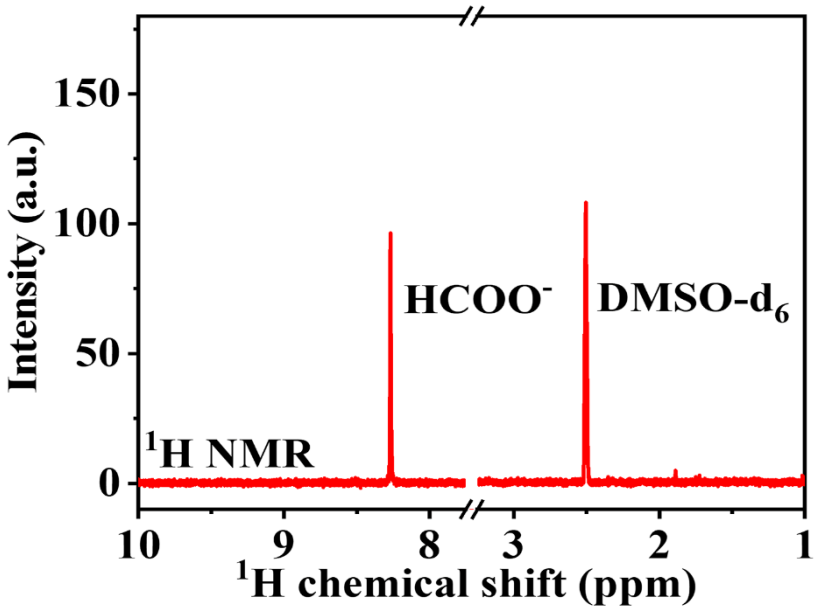

Fig. S13 The ^{1}H NMR of the product of CO_2RR by CA/3D-Cu biohybrid using DMSO-d_6 as an internal standard.

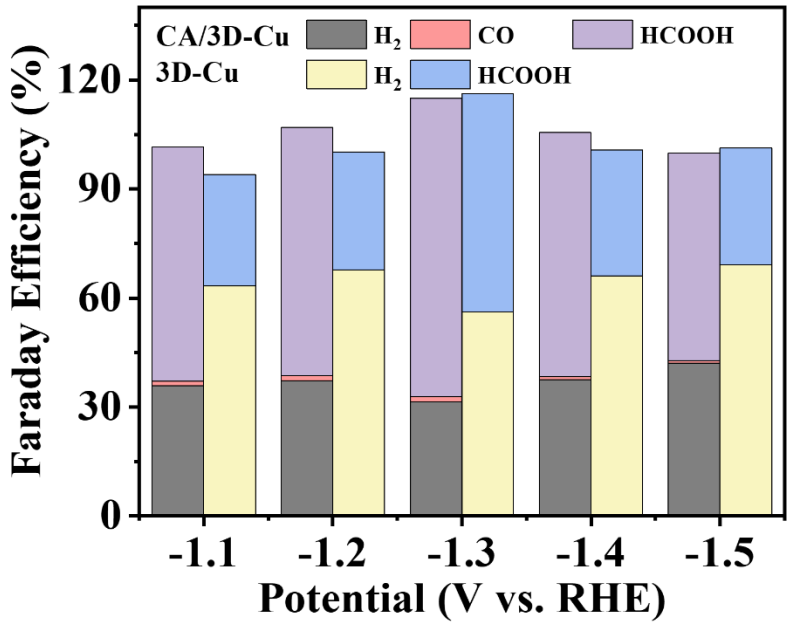

Fig. S14 FE of CO_2RR by CA/3D-Cu biohybrids and 3D-Cu at different potentials.

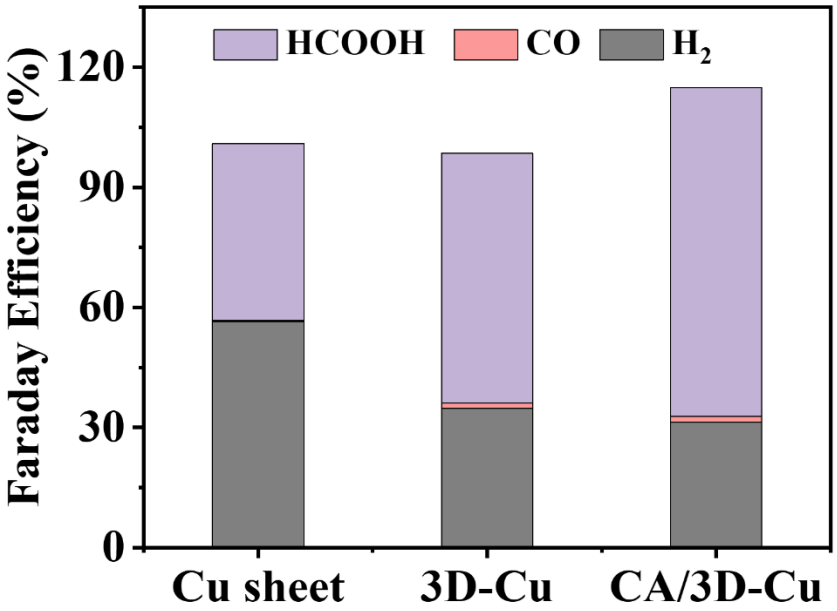

Fig. S15 FE of CO_2RR by Cu sheet, 3D-Cu, and CA/3D-Cu biohybrid at -1.3 V vs. RHE.

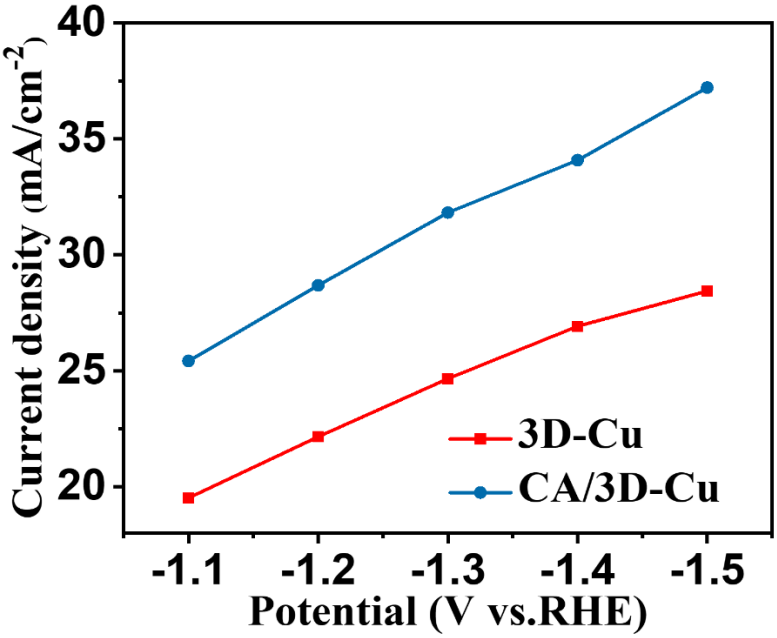

Fig. S16 Current densities of CO_2RR by CA/3D-Cu biohybrid and 3D-Cu at different potentials.

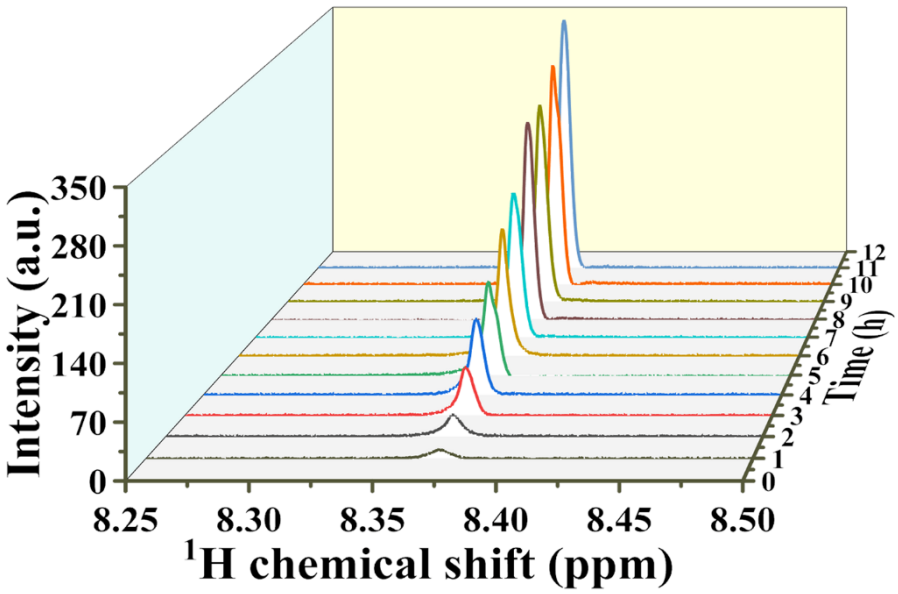

Fig. S17 ^{1}H NMR plots of formic acid at -1.3 V vs. RHE potential for different testing times.

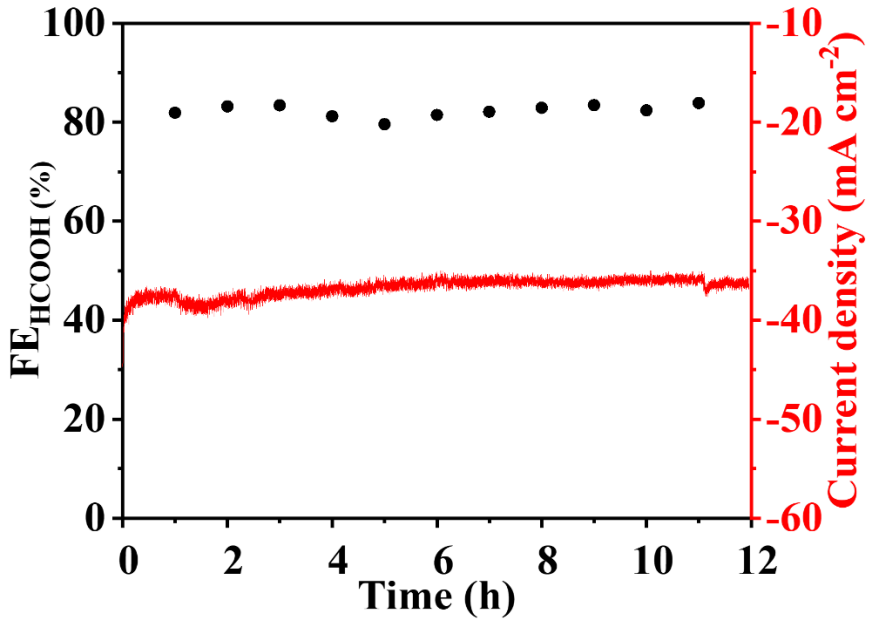

Fig. S18 Catalytic stability test of CA/3D-Cu biohybrid and FE_{HCOOH} for CO_2RR at -1.3 V vs. RHE for 12 h.

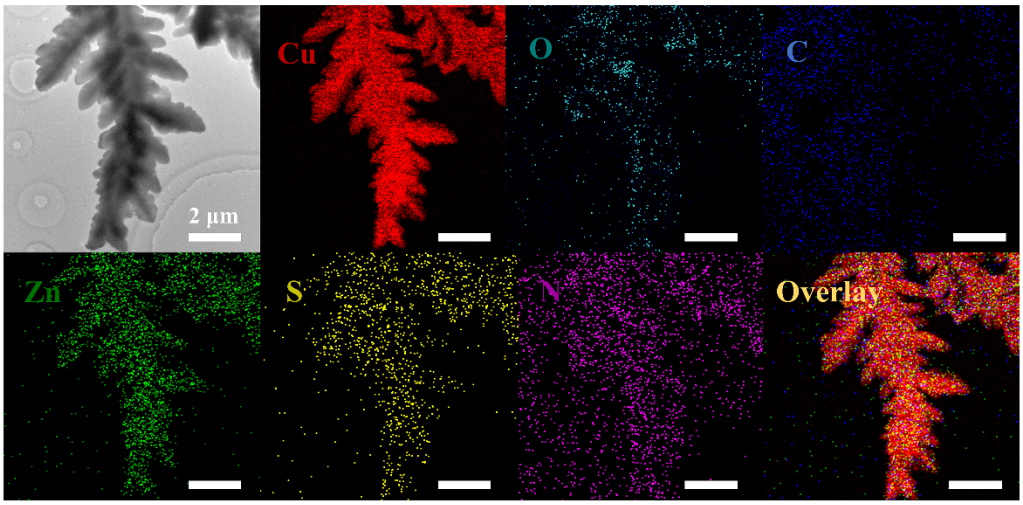

Fig. S19 TEM-EDX images of CA/3D-Cu biohybrid after chronoamperometry test for 12 h.

Notes and references

1 H. C. Shin and M. Liu, *Chem. Mater.*, 2004, **16**, 5460–5464.

2 T. N. Huan, P. Simon, G. Rousse, I. Génois, V. Artero and M. Fontecave, *Chem. Sci.*, 2016, **8**, 742–747.

3 S. C. Peter, *ACS Energy Lett.*, 2018, **3**, 1557–1561.

4 Y. Suzuki and K. Yokoyama, *Angew. Chem. Int. Ed.*, 2007, **119**, 4175–4177.

5 Z. Wang, Y. Kang, J. Hu, Q. Ji, Z. Lu, G. Xu, Y. Qi, M. Zhang, W. Zhang, R. Huang, L. Yu, Z. qun Tian and D. Deng, *Angew. Chem. Int. Ed.*, 2023, **2**, e202307086.

6 X. Guo, S. M. Xu, H. Zhou, Y. Ren, R. Ge, M. Xu, L. Zheng, X. Kong, M. Shao, Z. Li and H. Duan, *ACS Catal.*, 2022, **12**, 10551–10559.